

LETTER

Continuous time-resolved X-ray diffraction of the biocatalyzed reduction of Mn oxide

TIMOTHY B. FISCHER,<sup>1,\*</sup> PETER J. HEANEY,<sup>1</sup> JE-HUN JANG,<sup>2</sup> DANIEL E. ROSS,<sup>3</sup>  
SUSAN L. BRANTLEY,<sup>1</sup> JEFFREY E. POST,<sup>4</sup> AND MING TIEN<sup>3</sup>

<sup>1</sup>Department of Geosciences, Pennsylvania State University, University Park, Pennsylvania 16802, U.S.A.

<sup>2</sup>Penn State Institutes of Energy and the Environment, Pennsylvania State University, University Park, Pennsylvania 16802, U.S.A.

<sup>3</sup>Department of Biochemistry and Molecular Biology, Pennsylvania State University, University Park, Pennsylvania 16802, U.S.A.

<sup>4</sup>Department of Mineral Sciences, Smithsonian Institution, Washington, D.C. 20013, U.S.A.

ABSTRACT

Here we report the first continuous time-resolved X-ray diffraction analysis of a biologically mediated mineral reaction. We incubated total membrane (TM) fractions of the facultative anaerobe *Shewanella oneidensis* in an anoxic environmental reaction cell with formate (as electron donor via formate dehydrogenase) and powdered birnessite, a layered Mn<sup>3+,4+</sup> oxide common to many soils. Using both synchrotron and conventional X-ray sources, we irradiated the reaction mixtures for up to two weeks and observed bioreduction and dissolution of birnessite and the concomitant precipitation of rhodochrosite [Mn<sup>2+</sup>CO<sub>3</sub>] and hausmannite [Mn<sup>2+</sup>Mn<sub>2</sub><sup>3+</sup>O<sub>4</sub>]. The high time resolution of these experiments documented systematic changes in crystal structure during the breakdown of birnessite and the emergence of nanocrystalline rhodochrosite. In addition, the relative abundances of birnessite and rhodochrosite were quantified over time for different concentrations of TM fraction, allowing for the determination of rate equations that govern this bioreaction. Importantly, constant irradiation for two weeks did not stop the enzymatic reaction, suggesting that enzymes may be more resilient than whole cells when exposed to X-ray radiation.

**Keywords:** Mn oxide, biological-mineral interactions, time-resolved XRD, birnessite, rhodochrosite, hausmannite

INTRODUCTION

Bacteria play an integral role in the redox chemistry of the Earth's surface, and the biologically controlled generation and destruction of minerals have influenced surface processes since the earliest life forms emerged (Banfield and Nealson 1998; Hochella 2002; Weiner and Dove 2003). Over the last two decades researchers have documented bacterial respiration of solids for at least seven elemental systems [S, As, Se, Fe, U, C, and Mn (Lovley and Phillips 1988; Myers and Nealson 1988; Moser and Nealson 1996; Newman et al. 1997; Fredrickson et al. 2000; Bond et al. 2002; Herbel et al. 2003)]. Most investigations of solid-phase respiration have focused on electron transfer pathways between the crystal surface and the bacterial membrane, while the other side of the reaction—the evolution of the electronic state and crystallography of the solid—remains comparatively unexamined. Determining the rates and mechanisms of biomineralization processes requires a methodology that can record the structural evolution of nanocrystals during rapid growth, transformation, and dissolution. In many respects, X-ray diffraction (XRD) techniques are ideally suited to this task, especially in light of recent developments in imaging plate cameras and in the design of environmental reaction cells that allow real-time observation of mineral reactions in the presence

of fluids and gases (Parise et al. 2000; Lopano et al. 2007).

In the past, however, the application of X-ray diffraction to biomineralization has been thwarted by the lethal effects of intense X-rays on living systems. Doses from primary X-ray radiation range from 10<sup>3</sup> (sealed Cu tube) to 10<sup>7</sup> (synchrotron) rad/s, and direct exposure leads to cell death. To avoid this problem, researchers have collected diffraction data through brief irradiation episodes using mixtures of minerals and radiation-resistant bacterial spores or by analyzing the end products of batch reactions containing minerals and whole cells (Bargar et al. 2005; Setlow 2006; Coker et al. 2008). To assess bioreactions that are characterized by rapid precipitation of nanocrystals that structurally evolve during growth, however, continuous X-ray diffraction with high time resolution is required. We have developed a method that allows nearly uninterrupted collection of diffraction data during a biologically mediated reaction, and our results shed new light on the structural transformations that occur as minerals are bacterially dissolved and precipitated. These observations may help us understand the means by which electrons are transferred from bacterium to mineral during the process of dissimilatory bioreduction.

Our studies have focused on the reduction of synthetic birnessite [Na<sub>0.58</sub>(Mn<sub>1.42</sub><sup>4+</sup>, Mn<sub>0.58</sub><sup>3+</sup>)O<sub>4</sub>·1.5H<sub>2</sub>O], a layered Mn oxide found as a coating on soil particles in both arid and temperate climates, by the dissimilatory metal-reducing bacterium (DMRB) *Shewanella oneidensis* strain MR-1. Ruebush et al. (2006a,

\* E-mail: tfischer@geosc.psu.edu

2006b) demonstrated that Fe and Mn oxides can be reduced *in vitro* by the TM fractions of *S. oneidensis* by direct contact with the mineral surface. The TM fraction (composed of both outer and cytoplasmic membranes) contains formate-dehydrogenase and the required components for the transfer of electrons from formate (produced by catabolism of lactate) to the solid phase. Ruebush et al. (2006a, 2006b) followed oxide dissolution through the release of reduced  $\text{Fe}^{2+}$  and  $\text{Mn}^{2+}$  ions to solution and precipitation of a reduced metal carbonate phase. The *in vitro* model system used was well poised for time-resolved X-ray diffraction (TR-XRD) analysis because it contains the complete enzymatic machinery involved in bioreduction.

### EXPERIMENTAL METHODS AND RESULTS

XRD experiments were performed using both synchrotron radiation (National Synchrotron Light Source, Brookhaven National Laboratory) and a conventional sealed Mo tube source on a Rigaku II D/MAX-RAPID microdiffractometer. The reaction cell was modified after Small Environmental Cell for Real-Time Studies (SECRETS) (Parise et al. 2000). Reaction vessels consisted of 1 mm silica glass or single-crystal sapphire capillary tubes loaded with birnessite powder (crystal size  $<1 \mu\text{m}$ ), various concentrations of the TM fraction, and 1 M formate in 100 mM HEPES buffer at pH 7.4. The TM fraction was isolated and purified as in Ruebush et al. (2006a). Tubes were loaded in an anaerobic chamber and sealed with epoxy to maintain anoxia. For the synchrotron experiments, the reaction mixtures were frozen in liquid nitrogen (77 K) immediately after sealing and stored on dry ice (195 K) for transport to the beamline. Samples analyzed on the in-house device were sealed and placed immediately in the diffractometer. Because of differences in beam intensity, diffraction patterns of the reactant mixtures were collected every 4 min with synchrotron radiation and every 9 min with Mo radiation (Fig. 1).

The biodissolution of birnessite in response to the reduction of  $\text{Mn}^{4+}$  to  $\text{Mn}^{3+}$  and  $\text{Mn}^{3+}$  to  $\text{Mn}^{2+}$  is revealed in an abrupt loss of intensity of the (00 $l$ ) peaks (within the first minutes of reaction)

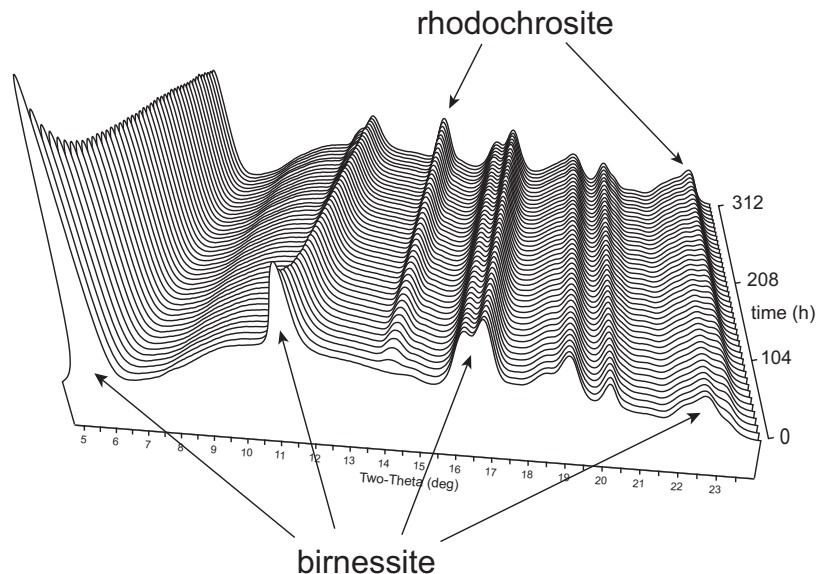
and a decrease in the refined unit-cell volume for birnessite by up to 1.3%. The contraction of the unit cell is due largely to a significant decrease in the *c*-axis, from 7.339(7) to 7.196(5) Å. In contrast, control experiments containing no TM produced no shift in the (001) and (002) peak positions. The decrease in *c* is caused almost exclusively by a thinning of the interlayer region in the reduced birnessite (Fig. 2). Interestingly, the refined occupancies of the octahedral Mn cations and of the interlayer atoms (modeled as O to proxy for disordered  $\text{H}_2\text{O}/\text{Na}$  species) (Post et al. 2002) showed little variation as dissolution proceeded. Thus, the enzymatically controlled reduction and electron transfer through the mineral induces a decreased layer charge that leads to the observed interlayer contraction.

As the dissolution of birnessite continued, rhodochrosite was observed to precipitate (Figs. 1 and 3). Ruebush et al. (2006a) demonstrated that dissolved  $\text{Mn}^{2+}$  is released by the bioreduction of birnessite, and we interpret the appearance of rhodochrosite as a response to saturation with respect to aqueous  $\text{Mn}^{2+}$  and  $\text{CO}_3^{2-}$ . The carbonate is generated by hydration of carbon dioxide, formed from the formate-dehydrogenase-catalyzed oxidation of formate. Formate is a metabolic product of lactate (Scott and Neelson 1994), a carbon source utilized by *Shewanella*. The precipitation of  $\text{MnCO}_3$  also serves to remove  $\text{Mn}^{2+}$  from the solution, thereby facilitating the continued reduction of Mn oxide. In one experiment, rhodochrosite precipitation ceased after 11 h and hausmannite ( $\text{Mn}_3\text{O}_4$ ) formed, probably due to the exhaustion of carbonate from the breakdown of formate. To our knowledge, this is the first evidence for the bioprecipitation of hausmannite.

Just as birnessite exhibited structural changes during reduction and dissolution, Rietveld analysis documented significant variations in the rhodochrosite structure as it nucleated and grew. Whereas the *a*-axis remained fairly constant with time, the *c*-axis decreased from 15.97 to 15.72 Å, a change of  $\sim 1.5\%$  (Fig. 2). The significant unit-cell contraction during the growth of the rhodochrosite crystals implies that the coarsening of these particles from nanoscale to micrometer grains is accompanied

by a striking decrease in the Mn-O-C bond angle. Scanning electron micrographs of the initial and final reaction solids reveal that these euhedral rhodochrosite rhombs achieved a final size of 5  $\mu\text{m}$  and were mixed with birnessite. Birnessite crystals transformed from a mixture of bladed and platy crystals to hexagonal platelets.

The time-resolution of these experiments allowed for the determination of the rate of bioprecipitation of rhodochrosite ( $\text{Rate} = dM_{\text{Rhod}}/dt$ ), where  $M_{\text{Rhod}}$  repre-



◀ **FIGURE 1.** Stacked diffraction patterns showing birnessite biodissolution and rhodochrosite bioprecipitation in solutions with 1 M formate and 2.0 mg/mL TM fraction at pH 7.5. Each diffraction pattern represents a 9 min interval. The data shown were acquired on a Mo source diffractometer.

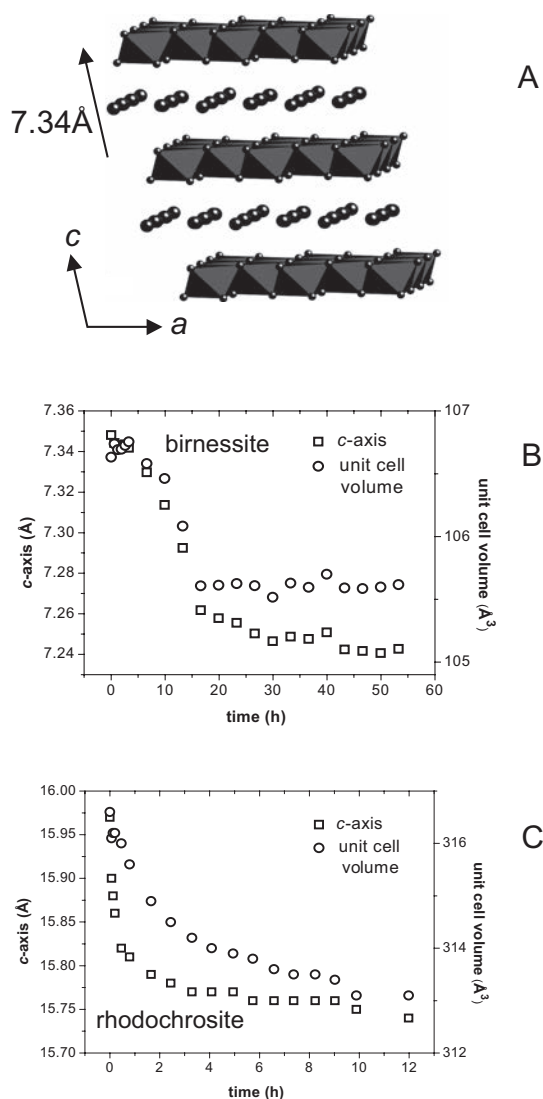


**FIGURE 2.** Projection of the structure for starting synthetic birnessite (a). O atoms are shown at the corners of the octahedra and interlayer Na/H<sub>2</sub>O are shown as individual atoms. Changes in the *c*-unit cell parameter (squares) and unit cell volume (circles) of synthetic birnessite (b) and bioprecipitated rhodochrosite (c) as bioreduction occurred in solutions with 1 *M* formate at pH 7.5. Calculated errors are smaller than the symbols.

sents the normalized mass abundance of rhodochrosite and was calculated by exploiting the proportional relationship between refined diffraction scale factors and phase abundances. All experiments revealed two distinct reaction stages. As shown by the dependence of rhodochrosite concentrations with time (Fig. 3), fast initial nucleation was followed by slow growth. As expected given the high concentrations of birnessite and formate in the starting solutions, the rates of reaction are relatively insensitive to variations in birnessite and formate concentration. However, the rates vary with the concentration of total membrane fraction according to the following first-order rate equation,

$$\text{Rate} = k [\text{TM}] \quad (1)$$

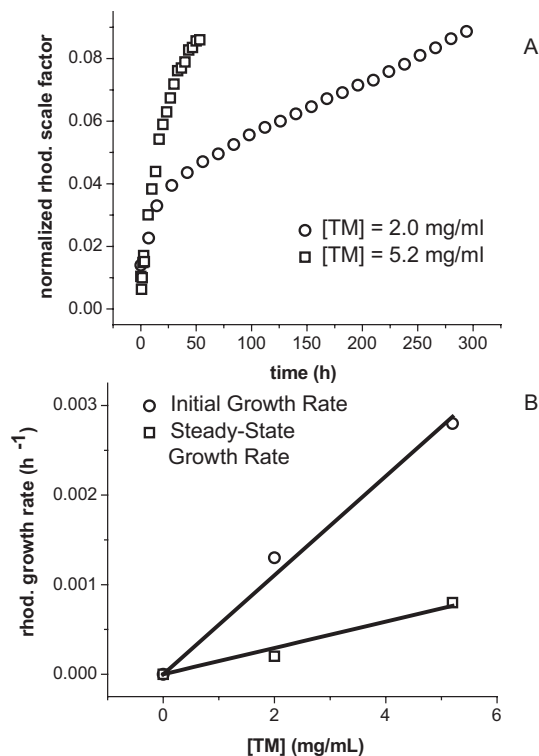


**FIGURE 3.** Changes in the normalized mass abundance of rhodochrosite during bioreaction (a) and the dependence of rhodochrosite growth rate on TM concentration (b). Normalized mass abundances are calculated by dividing the rhodochrosite scale factor by the initial birnessite scale factor. Circles represent an experiment with 1 *M* formate and 2.0 mg/mL TM fraction at pH = 7.5; squares represent an experiment with 1 *M* formate and 5.2 mg/mL TM fraction at pH = 7.5. Circles represent initial nucleation rates ( $R^2 = 0.9917$ ) and squares represent steady-state growth rates ( $R^2 = 0.9781$ ).

where  $k$  is a rate constant and [TM] is the concentration of the total membrane in mg/mL. Our analysis revealed that  $k$  was  $6 \times 10^{-4}$  mL/(mg·h) for the nucleation stage, but slowed to  $1 \times 10^{-4}$  mL/(mg·h) (Fig. 3).

These experiments yield insights into the fate of Mn solids that participate in DMRB reactions, and they suggest that Mn within birnessite is reduced prior to dissolution, generating transient intermediate phases with a collapsing interlayer structure. Although these experiments did not employ living bacteria, they demonstrate that one can extract the enzymes responsible for biologically controlled redox reactions and analyze the reactions in real-time by diffraction methods. We have shown that the enzymes continue to function at continuous, high radiation doses for periods of 2 weeks in a Mn oxide system. Daly et al. (2007) argued that the redox cycling of Mn<sup>2+</sup> in ionizing radiation (IR) resistant bacteria protects proteins from oxidation, whereas the reduction of Fe<sup>3+</sup> oxides to Fe<sup>2+</sup> will produce reactive oxygen species that can damage proteins. Therefore this experimental system may not be as robust when applied to Fe oxide systems. Nevertheless, we regard TR-XRD as a novel and robust means of interrogating bioreactions to obtain coupled insights into their

mechanisms, kinetics, and the corresponding structural changes of mineral phases involved in the bioreaction.

#### ACKNOWLEDGMENTS

Funding for this research was provided the following grants: NSF grant EAR04-17741; the Biogeochemical Research Initiative for Education (BRIE), an NSF IGERT grant (DGE-9972759); the Center for Environmental Kinetics Analysis (CEKA), an NSF- and DOE-sponsored Environmental Molecular Science Institute (NSF CHE-0431328). This research was carried out at the National Synchrotron Light Source, Brookhaven National Laboratory, which is supported by the U.S. Department of Energy, Division of Materials Sciences and Division of Chemical Sciences, under Contract No. DE-AC02-98CH10886.

#### REFERENCES CITED

- Banfield, J.F. and Nealson, K.H., Eds. (1998) *Geomicrobiology: Interactions Between Microbes and Minerals*, vol. 35. Reviews in Mineralogy, Mineralogical Society of America, Chantilly, Virginia.
- Bargar, J.R., Tebo, B.M., Bergmann, U., Webb, S.M., Glatzel, P., Chiu, V.Q., and Villalobos, M. (2005) Biotic and abiotic products of Mn(II) oxidation by spores of the marine *Bacillus sp.* strain SG-1. *American Mineralogist*, 90, 143–154.
- Coker, V.S., Bell, A.M.T., Pearce, C.I., Patrick, R.A.D., van der Laan, G., and Lloyd, J.R. (2008) Time-resolved synchrotron powder X-ray diffraction study of magnetite formation by the Fe(III)-reducing bacterium *Geobacter sulfurreducens*. *American Mineralogist*, 93, 540–547.
- Daly, M.J., Gaidamakova, E.K., Matrosova, V.Y., Vasilenko, A., Zhai, M., Leapman, R.D., Lai, B., Ravel, B., Li, S.-M.W., Kemner, K.M., and Fredrickson, J.K. (2007) Protein oxidation implicated as the primary determinant of bacterial radioresistance. *Public Library of Science (PLoS) Biology*, 5, e92, DOI: 10.1371/journal.pbio.0050092.
- Fredrickson, J.K., Zachara J.M., Kennedy, D.W., Duff, M.C., Gorby, Y.A., Li, S.M.W., and Krupka, K.M. (2000) Reduction of U(VI) in goethite ( $\alpha$ -FeOOH) suspensions by a dissimilatory metal-reducing bacterium. *Geochimica et Cosmochimica Acta*, 64, 3085–3089.
- Herbel, M.J., Blum, J.S., Oremland, R.S., and Borglin, S.E. (2003) Reduction of elemental selenium to selenide: Experiments with anoxic sediments and bacteria that respire Se-oxyanions. *Geomicrobiology Journal*, 20, 587–602.
- Hochella, M.F. (2002) Sustaining Earth: Thoughts on the present and future roles of mineralogy in environmental science. *Mineralogical Magazine*, 66, 627–652.
- Lopano, C.L., Heaney, P.J., Post, J.E., Hanson, J., and Komarneni, S. (2007) Time-resolved structural analysis of K- and Ba-exchange reactions with synthetic Na-birnessite using synchrotron X-ray diffraction. *American Mineralogist*, 92, 380–387.
- Lovley, D.R. and Phillips, E.J.P. (1988) Novel mode of microbial energy metabolism: Organic carbon oxidation coupled to dissimilatory reduction of iron or manganese. *Applied and Environmental Microbiology*, 54, 1472–1480.
- Moser, D.P. and Nealson, K.H. (1996) Growth of the facultative anaerobe *Shewanella putrefaciens*. *Applied and Environmental Microbiology*, 62, 2100–2105.
- Myers, C.R. and Nealson, K.H. (1988) Microbial reduction of manganese oxides: Interactions with iron and sulfur. *Geochimica et Cosmochimica Acta*, 52, 2727–2732.
- Newman, D.K., Kennedy, E.K., Coates, J.D., Ahmann, D., Ellis, D.J., Lovley, D.R., and Morel, F.M.M. (1997) Dissimilatory arsenate and sulfate reduction in *Desulfotomaculum auripigmentum sp. nov.* *Archives of Microbiology*, 168, 380–388.
- Parise, J.B., Cahill, C.L., and Lee, Y.J. (2000) Dynamic powder crystallography with synchrotron X-ray sources. *Canadian Mineralogist*, 38, 777–800.
- Post, J.E., Heaney, P.J., and Hanson, J. (2002) Rietveld refinement of a triclinic structure for synthetic Na-birnessite using synchrotron powder diffraction data. *Powder Diffraction*, 17, 218–221.
- Ruebush, S.S., Icopini, G.A., Brantley, S.L., and Tien, M. (2006a) In vitro enzymatic reduction kinetics of mineral oxides by membrane fractions from *Shewanella oneidensis* MR-1. *Geochimica et Cosmochimica Acta*, 70, 56–70.
- Ruebush, S.S., Brantley, S.L., and Tien, M. (2006b) Reduction of soluble and insoluble iron forms by membrane fractions of *Shewanella oneidensis* grown under aerobic and anaerobic conditions. *Applied and Environmental Microbiology*, 72, 2925–2935.
- Scott, J.H. and Nealson, K.H. (1994) A biochemical study of the intermediary carbon metabolism of *Shewanella putrefaciens*. *Journal of Bacteriology*, 176, 3408–3411.
- Setlow, P. (2006) Spores of *Bacillus subtilis*: Their resistance to and killing by radiation, heat and chemicals. *Journal of Applied Microbiology*, 101, 514–525.
- Weiner, S.S. and Dove, P.M. (2003) An overview of biomineralization processes and the problem of the vital effect. In P.M. Dove, J.J. De Yoreo, and S. Weiner, Eds. *Biomineralization*, 54, p. 1–29. Reviews in Mineralogy and Geochemistry, Mineralogical Society of America, Chantilly, Virginia.

MANUSCRIPT RECEIVED JUNE 6, 2008

MANUSCRIPT ACCEPTED AUGUST 9, 2008

MANUSCRIPT HANDLED BY BRYAN CHAKOUMAKOS